POLITECNICO DI TORINO
Repository ISTITUZIONALE

Characterization of the Frequency Dependence of Impedance standards with a Dual Josephson Impedance Bridge

Original
Characterization of the Frequency Dependence of Impedance standards with a Dual Josephson Impedance Bridge / Medved, J., Overney, F., Ortolano, M.. - ELETTRONICO. - (2026). (2026 Conference on Precision Electromagnetic Measurements (CPEM 2026) Madrid (Spa) 06-11 September 2026).

Availability:
This version is available at: 11583/3015534 since: 2026-09-15T17:50:23Z

Publisher:
IEEE

Published
DOI:

Terms of use:

This article is made available under terms and conditions as specified in the corresponding bibliographic description in the repository

Publisher copyright
IEEE postprint/Author's Accepted Manuscript

©2026 IEEE. Personal use of this material is permitted. Permission from IEEE must be obtained for all other uses, in any current or future media, including reprinting/republishing this material for advertising or promotional purposes, creating new collecting works, for resale or lists, or reuse of any copyrighted component of this work in other works.

(Article begins on next page)

18 November 2026

Characterization of the Frequency Dependence of Impedance standards with a Dual Josephson Impedance Bridge

Juan Medved[1, 2], Frédéric Overney[3], and Massimo Ortolano[2]
[1]Istituto Nazionale di Ricerca Metrologica (INRIM), Turin, Italy
j.medved@inrim.it
[2]Politecnico di Torino (POLITO), Turin, Italy
[3]Federal Institute of Metrology (METAS), Bern, Switzerland

***Abstract*—In this work, the frequency dependence of impedance standards is characterized using a quantum-based impedance bridge. The $1:1$ ratio of two quadrifilar calculable resistance standards and the impedance of a $1\,\mathrm{nF}$ capacitance standard are measured from $180\,\mathrm{Hz}$ to $80\,\mathrm{kHz}$. At $1233\,\mathrm{Hz}$ the combined standard uncertainty is $30\,\mathrm{nF/F}$ for the relative capacitance and $2.5\,\mathrm{n\Omega/\Omega}$ for the resistance ratio, demonstrating the unique capability of the bridge for accurate impedance standards characterization.**

***Index Terms*—Bridge circuits, impedance measurement, measurement techniques, precision measurements.**

I. Introduction

Traditional impedance bridges rely on ratio transformers to generate the accurate voltage ratios required for high-accuracy impedance measurements. However, the use of a fixed-ratio transformer limits the types of impedance comparisons that can be performed, as well as the frequency range and impedance ratio. As a consequence, the frequency characterization of impedance standards using traditional bridges is time-consuming and can only be carried out at a limited number of frequency points and impedance values [1]–[3].

In recent years, impedance bridges employing electronic sources rather than ratio transformers have been developed and validated through international comparisons [4]. These bridges can generate arbitrary voltage ratios and phase shifts, allowing for comparisons of any impedance in the complex plane and broader frequency ranges. In addition, the replacement of electronic sources with quantum-based sources, such as the *Josephson arbitrary waveform synthesizer* (JAWS), allows impedance measurements to be performed at the highest level of accuracy [5].

In this work, a *dual Josephson impedance bridge* (DJIB) developed at METAS [6], [7] is used to study the frequency dependence of resistance and capacitance standards. Measurements of similar and unlike impedance standards in *direct* and *reverse* configuration were performed, covering impedance ratios from $0.1:1$ to $1:10$. The standards were reversed at the bridge panel level using cables of the same length. The maximum rms amplitude used in this work is $250\,\mathrm{mV}$ from $180\,\mathrm{Hz}$ to $80\,\mathrm{kHz}$.

II. Impedance Comparisons

Five different impedance standards have been used in the different impedance comparisons shown in Fig. 1:

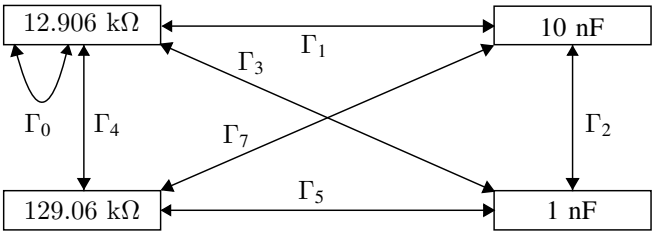


Figure 1. Impedance standards and bridge ratios Γ used in this work.

- Two quadrifilar calculable resistance standards having the same nominal value of $12.906\,\mathrm{k\Omega}$.
- One resistance standard of $129.06\,\mathrm{k\Omega}$ with a commercial Vishay resistive element of type VHP101.
- Two capacitance standards of $1\,\mathrm{nF}$ and $10\,\mathrm{nF}$ designed by the Polish National Metrology Institute and made of commercial single C0G SMD capacitors [8].

All standards are individually temperature controlled and defined as four-terminal-pair standard.

The impedance of a resistance standard is usually represented as $Z = R/(1 - \mathrm{j}\omega\tau)$, where R is the parallel equivalent resistance and τ the time constant. The impedance of a capacitance standard is usually represented as $Y = Z^{-1} = \mathrm{j}\omega C(1 - \mathrm{j}D)$ where C is the capacitance value and D the dissipation factor. Operating the DJIB, the impedance ratio

$$\Gamma = \frac{Z_{\mathrm{bot}}}{Z_{\mathrm{top}}} = -\frac{V_{\mathrm{bot}}}{V_{\mathrm{top}}} \tag{1}$$

can be determined for different impedance comparison [6].

Fig. 1 shows the possible impedance comparisons between the available standards and Table I summarizes the type of comparison, impedance ratio, and frequency range of each

Table I
Impedance comparisons.

Comparison	Type	Ratio	Frequency range
Γ_0	RR	1:1	180 Hz – 80 kHz
Γ_4	RR	1:10	180 Hz – 80 kHz
Γ_1	RC	0.1:10	180 Hz – 10 kHz
Γ_3	RC	0.1:10	1233 Hz – 80 kHz
Γ_5	RC	0.1:10	180 Hz – 10 kHz
Γ_7	RC	0.1:10	180 Hz – 1233 Hz
Γ_2	CC	1:10	180 Hz – 80 kHz

979-8-3315-4683-0/26/$31.00 ©2026 IEEE

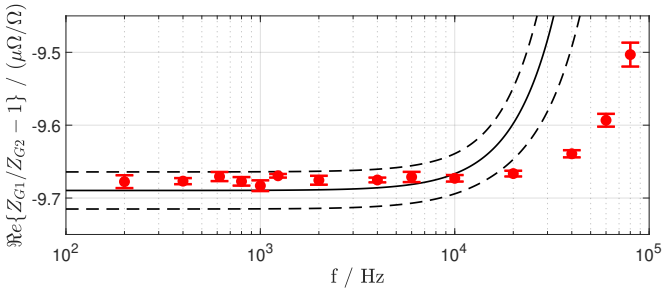


Figure 2. Comparison Γ_0 between two quadrifilar calculable resistance standards of 12 906 Ω. In red, the deviation of the nominal ratio. Solid black lines represent the calculated values using Eq. (2). The uncertainty bars represent the combined standard uncertainty ($k = 1$).

case. For each comparison, the frequency range was limited to keep impedance ratio between $0.1:1$ and $1:10$ for which the bridge had previously been characterized.

III. Results

The result of the $1:1$ comparison Γ_0 of the two quadrifilar calculable resistance standards G_1 and G_2 over the whole frequency range is represented in Fig. 2. As G_1 and G_2 have the same design, one would expect no frequency dependence of the impedance ratio, contrary to what is observed. However, a more detailed analysis of the real part of the measured impedance ratio is obtained using the equivalent expression for the two impedance standards. The real part of Γ_0 is

$$\mathrm{Re}\{\Gamma_0\} = \mathrm{Re}\left\{\frac{Z_{\mathrm{G1}}}{Z_{\mathrm{G2}}}\right\} = \frac{R_{\mathrm{G1}}}{R_{\mathrm{G2}}}\,\frac{1+\omega^2\tau_{\mathrm{G2}}\tau_{\mathrm{G1}}}{1+\omega^2\tau_{\mathrm{G1}}^2}. \qquad (2)$$

Therefore, even if the two resistance elements have the same frequency dependence (i.e. $R_{\mathrm{G1}}/R_{\mathrm{G2}} = \text{const.}$), $\mathrm{Re}\{\Gamma_0\}$, could show a frequency dependence if $\tau_{\mathrm{G1}} \neq \tau_{\mathrm{G2}}$. The origin of the remaining difference between the measured and calculated values, as observed above 20 kHz in Fig. 2, could be due to the fixed cables inside the case of the standards.

The frequency dependence of C and D of the 1 nF standard is shown in Fig. 3. C is expressed as the relative deviation with respect to its value at the reference frequency $f_0 = 1233$ Hz. This frequency dependence is determined using three alternative comparisons between the impedance standards. The RC comparison between G_2 and the 1 nF capacitor, Γ_3, is represented as orange triangles. The behavior at lower frequencies is obtained by combining the RC comparison between G_2 and the 10 nF capacitor, Γ_1, with the 1:10 comparison between the 1 nF and 10 nF standards, Γ_2. These results are shown as blue dots. The low frequency part is also obtained from the combination of the 1:10 comparison between G_2 and the Vishay resistor , Γ_4, and the RC comparison between this latter resistor and the 1 nF capacitor, Γ_5. This path is represented by green squares. Least-squares fits are shown as solid black lines, using the model $a + bf^2 + c\log_{10}(f)$ for C [2].

At 180 Hz the relative deviation of C is about 3.40(12) µF/F for Γ_3 and 3.22(21) µF/F for $\Gamma_4\Gamma_5$. As the frequency increases, the relative deviation decreases and reaches a minimum close to 40 kHz, where it is about −4.80(14) µF/F. At higher frequencies it increases again,

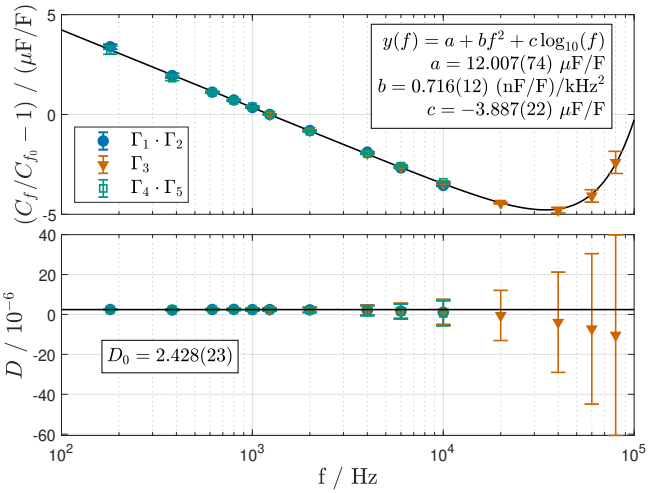


Figure 3. Frequency dependence of the 1 nF capacitor. Upper: capacitance C as the relative deviation from its value at $f_0 = 1233$ Hz. Lower: dissipation factor D. Three comparison paths $\Gamma_1\Gamma_2$ (blue dots), Γ_3 (orange triangles) and $\Gamma_4\Gamma_5$ (green squares), and least-square fits (solid black lines) are shown. Error bars represent the combined standard uncertainty ($k = 1$).

reaching −2.40(55) µF/F at 80 kHz, possibly due to lead inductance effects in the standard. In contrast, D is constant over the whole frequency range, with a best-fit value of $D_0 = 2.428(23) \times 10^{-6}$. The combined standard uncertainty was calculated as described in [6]. For C at f_0 it is 0.030 µF/F.

IV. Conclusion

The unique ability of the DJIB to measure any impedance in the complex plane allowed us to characterize the frequency dependence of resistance and capacitance standards over a broad frequency range using the same experimental setup. For the 1 nF capacitance standard, the frequency dependence obtained from the different impedance comparisons is mutually consistent and in agreement with previous work.

References

[1] F. Delahaye and R. Goebel, "Evaluation of the Frequency Dependence of the Resistance and Capacitance Standards in the BIPM Quadrature Bridge," *IEEE Transactions on Instrumentation and Measurement*, vol. 54, no. 2, pp. 533–537, 4 2005.

[2] Y. Wang, "Frequency dependence of capacitance standards," *Review of Scientific Instruments*, vol. 74, no. 9, pp. 4212–4215, 2003.

[3] Y. Wang and S. H. Shields, "Improved capacitance measurements with respect to a 1-pF Cross-capacitor from 200 to 2000 Hz," *IEEE Transactions on Instrumentation and Measurement*, vol. 54, no. 2, pp. 542–545, 2005.

[4] M. Ortolano *et al.*, "An international trilateral comparison among the newest generations of digital and josephson impedance bridges," *IEEE Trans. Instrum. Meas.*, 2025.

[5] F. Overney and B. Jeanneret, "Impedance bridges: from Wheatstone to Josephson," *Metrologia*, vol. 55, no. 5, pp. S119–S134, 10 2018.

[6] F. Overney *et al.*, "Dual Josephson impedance bridge: towards a universal bridge for impedance metrology," *Metrologia*, vol. 57, no. 6, p. 065014, 12 2020.

[7] Y. Pimsut *et al.*, "Development and implementation of an automated four-terminal-pair Josephson impedance bridge," *Metrologia*, vol. 61, no. 2, p. 025007, 4 2024.

[8] K. Musioł, M. Koszarny, M. Kampik, K. Kubiczek, A. Ziółek, and J. Jursza, "A New Impedance Metrology Infrastructure at GUM," in *Proceedings of the 25th IMEKO TC4 International Symposium and 23rd International Workshop on ADC and DAC Modelling and Testing*, vol. 21. Budapest: IMEKO, 2022, pp. 243–247.